

# A Variable-Gain Low-Noise Amplifier for MedRadio Band Applications

Mutanizam Abdul Mubin<sup>1</sup>, Mohd Tafir Mustaffa<sup>1,\*</sup>, and Arjuna Marzuki<sup>2</sup>

<sup>1</sup> School of Electrical and Electronic Engineering, Universiti Sains Malaysia, 14300 Nibong Tebal, Malaysia

<sup>2</sup> School of Science and Technology, Wawasan Open University, 10050 George Town, Malaysia

Email: mutanizam@student.usm.my (M.A.M.), tafir@usm.my (M.T.M.), arjunam@wou.edu.my (A.M.)

**Abstract**—A variable-gain 0.18  $\mu\text{m}$  Complementary Metal-Oxide-Semiconductor (CMOS) Low-Noise Amplifier (LNA) for Medical Device Radiocommunications Service (MedRadio) applications has been designed and verified through simulations in Cadence IC5 with Silterra's C18G CMOS technology Process Design Kit. Unlike other MedRadio LNAs from previous works, this proposed LNA can vary its gain from just above 10 dB to nearly 30 dB. It consists of three stages; the input-matching stage, the inter-stage buffer, and the gain-varying stage. The input-matching stage provides an input impedance match and drives the initial gain of the LNA. The inter-stage buffer isolates the input-matching stage from the gain-varying stage. The overall gain of the LNA can be varied and is determined by the variable biasing of the driving transistors of the gain-varying stage. On post-layout simulations with a source-follower output buffer, this LNA exhibits a wide-ranging gain from 11.2 dB at 0.49 mW DC power consumption to 29.1 dB at 1.34 mW DC power consumption.

**Index Terms**—Low-Noise Amplifier (LNA), Medical Device Radiocommunications Service (MedRadio), variable-gain

## I. INTRODUCTION

In today's world, affordable and economical medical services are getting more and more important due to the increase in global life expectancy. Consequently, extensive research and development activities in the field of wireless communications specifically for biomedical purposes are growing rapidly. These activities have since paved the way for the development and introduction of some state-of-the-art biomedical devices such as remote-controlled cardiac pacemakers and implants for drug delivery [1]. These implantable biomedical devices promote patients' independence and enable them to carry on with their lives like ordinary people [2]. One of the most common frequency bands to be utilized for wireless communications of these medical devices is the Medical Device Radiocommunications Service (MedRadio) frequency spectrum that spans from 401 MHz to 406 MHz [3, 4]. Other frequency band options for wireless communications of biomedical devices include the European Short-Range Radio Device (SRD) band between 868 MHz to 928 MHz and the Industrial Scientific Medical

(ISM) band around 2.4 GHz. However, unlike these two bands, the MedRadio frequency spectrum is solely dedicated to biomedical applications thus making it much more suitable for wireless communications of biomedical devices as compared to the ISM and SRD bands [5].

The Low-Noise Amplifier (LNA) is usually the first active block in the receiver section of a general wireless communication system [6]. It must therefore provide sufficient gain to amplify signals received at the antenna and at the same time minimize the amount of added noise. A very low noise figure value for the LNA is desired since it is the first active stage in the receiver chain. To minimize the noise contribution of subsequent stages after the LNA, the gain of the LNA must be significantly large [6]. The LNA should also be capable of limiting distortions when handling relatively large input signals. To obtain maximum power transfer into the LNA, a suitable input impedance, which is usually  $50 \Omega$ , must be presented at its input. For MedRadio applications, it is extremely important for the LNA in the receiver front-end of a biomedical device to consume as little power as possible. This is to prolong battery life to reduce the frequency of surgery for battery replacement hence providing more stability, reliability, and cost-efficiency for the biomedical device [7]. However, operating at very low power may compromise the gain and noise figure of the LNA thus affecting the signal transmission through the receiver chain and degrading the whole communication system performance [8]. Hence, the main challenge in the design and development of a MedRadio LNA is to obtain a suitable trade-off between the gain, noise figure, and DC power consumption of the LNA. In addition, a very small physical size of the LNA integrated circuit (IC) is desirable to minimize the overall size of the receiver front-end and the biomedical device as a whole. This is for convenience as the biomedical devices are to be body-worn or embedded underneath the skin of the patient [9].

The sensitivity of an RF (Radio-Frequency) receiver is defined as the minimum input power that is required for detection by the receiver. Link budget analyses done by previous works such as [5, 10, 11] suggested sensitivity values of  $-90 \text{ dBm}$  to  $-97 \text{ dBm}$  for RF receivers of MedRadio devices. With these very low input power levels, the gain of the LNA must be adequately high to amplify the input signal before the down-conversion by the mixer. Reference [11] proposed a gain specification of greater

Manuscript received January 8, 2024; revised April 3, 2024; accepted April 18, 2024.

\*Corresponding author

than 35 dB which was considerably very high. Reference [10] however, suggested a much more relaxed gain specification of just over 10 dB. The sensitivity of a MedRadio receiver was also used to determine the required noise figure of the receiver. From a sensitivity of around  $-90$  dBm, Reference [11] estimated a value of approximately 19 dB for the overall noise figure of a MedRadio receiver. Reference [5] however, suggested a much lower overall noise figure value of 12 dB to allow for sensitivity of  $-97$  dBm. Since the LNA is the first active component of the receiver, the noise figure of the LNA should be lowered to as low as possible. For input return loss, 10 dB is commonly accepted as the minimum level in RF and microwave systems to reduce the amount of reflected signal. With a maximum transmitted power of  $-16$  dBm, MedRadio signals are typically very low and weak RF signals. At the receiver input, the maximum received power is estimated to be just around  $-30$  dBm due to the minimum communication distance of 20 cm for health-monitoring applications [11]. Hence, the linearity for MedRadio LNAs should not be much of a concern as long as the LNA does not start to saturate below  $-30$  dBm of input power level. Therefore,  $-30$  dBm (or greater) should be the suitable target for the input 1-dB compression point ( $IP_{1dB}$ ). The input third-order intercept point ( $IIP_3$ ) is related to  $IP_{1dB}$  by [12]:

$$IIP_3 = IP_{1dB} + 9.6 \text{ dB} \quad (1)$$

Previous works on MedRadio LNA seemed to be directed towards finding the optimum balance amongst all the aforementioned LNA parameters [5, 9, 11, 13]. The LNAs in these works operated with fixed DC conditions that focused on low DC power consumption with high gain, low noise figure, and also acceptable linearity and input return loss. In actual fact, the DC power consumption could have been further reduced when the input signal power level was significantly higher than the sensitivity of the receiver. In this condition, the LNA gain requirement could have been relaxed, hence lower DC power consumption with lower gain could be afforded. On the contrary, in cases where the input signal was very weak and the input power level was only slightly higher than the receiver's sensitivity, a much higher gain would be needed and this would require the DC power consumption to be increased. All in all, the LNA could have been more efficient if the gain and DC power consumption were not fixed and could be adjusted according to the strength of the input signal at the receiver. Hence, the objective of this work is to propose a variable-gain LNA integrated circuit for MedRadio applications. The gain-variability of this LNA will also be very useful to counteract the effect of process variations and mismatches of the IC, hence improving the yield.

This paper describes the circuit design and analysis of a variable-gain LNA for MedRadio applications together with its post-layout simulation results and discussions. Section II of this paper reviews some previous works on variable-gain LNAs. The circuit design and analysis of the proposed variable-gain MedRadio LNA are described in Section III. Section IV presents the post-layout simulation

results and some discussions of the results. Section V concludes this work. In this work, Silterra's  $0.18 \mu\text{m}$  CMOS technology is employed.

## II. PREVIOUS REPORTED VARIABLE-GAIN LNAs

To the best of the authors' knowledge, no such variable-gain MedRadio LNA has been reported to date. Reference [14] however, proposed a complementary metal-oxide-semiconductor (CMOS) reconfigurable MedRadio receiver front-end with 3 operational modes; active-matching mode, variable-gain mode, and LNA-bypass mode. Although some raw simulation results were provided, this work, however, focused more on the architectural level without going into too much detail on the circuits involved. There was also no physical implementation in the form of an IC layout. The emphasis of this work was generally on providing a wide-range energy-performance scalability study. It was not providing an integrated circuit solution for a receiver front-end of MedRadio biomedical devices. The receiver front-end in this work consisted of an LNA, a passive mixer, and a differential ring oscillator. The variable-gain mode worked at the LNA level. In this mode, the LNA gain could be adjusted through two methods. The first method was by varying the total width of the LNA's CMOS transistors which caused a change in total current through the transistors. This was implemented by connecting LNA cells of the same size in parallel. With this parallel structure, the total transistor width of the LNA could be reconfigured by turning on different numbers of LNA cells. This method of varying the gain and DC power consumption did not seem to be very feasible since having several LNAs connected in parallel would take up a significant amount of space in the IC. This would result in a very bulky and space-consuming receiver front-end and hence might not be suitable for biomedical devices. The second method was by tweaking the gate-biasing voltage of the LNA transistors to vary the current through the transistors. Even though the current was very sensitive to the gate-biasing voltage, this method of adjusting the gain and DC power consumption seemed to be more practical and realistic in terms of the physical realization of the IC, compared to the first method.

Although no such variable-gain MedRadio LNA has been reported thus far, several published works on general variable-gain LNA are available in the literature. The work in [15] presented a  $0.6 \text{ mW}$   $0.18 \mu\text{m}$  CMOS variable-gain LNA with an operating frequency of 2.8 GHz. In this work, the LNA was capable of varying its gain from 4 dB to 10 dB. A  $0.18 \mu\text{m}$  CMOS variable-gain LNA for  $0.18 \mu\text{m}$  3.5 GHz to 9 GHz ultra-wideband applications was proposed by [16]. The gain variation of this LNA was from 6 dB to 12 dB at 14 mW constant DC power consumption. In [17], a 0.3 GHz to 1.4 GHz inductorless CMOS variable-gain LNA was described. The gain for this LNA could be varied from  $-24.9$  dB to 21 dB with an unchanged DC power consumption of 8 mW. For all these three works, the purpose of gain variation was to maintain the linearity of the LNA by preventing large input signals from saturating the LNA. In all these 3 works, gain variation was achieved

by tuning the gate-biasing voltage of the MOS transistor in the feedback path, and this did not cause any change in the total DC power consumption of the LNA. Hence, for these 3 works, the variable-gain function was not for power-saving when the input signal is large. In addition, the operating frequency ranges of [15] and [16] and the relatively high DC power consumption of [16] and [17] were not suitable for MedRadio applications.

### III. CIRCUIT DESIGN AND ANALYSIS

#### A. Topology and Structure

The work from [13] had proven the effectiveness of the complementary common-source current-reuse topology with active shunt feedback in producing an LNA circuit with generally acceptable overall performance for MedRadio applications. This topology, however, may only be suitable for a fixed gain value. This is because for this topology, varying gain changes the input impedance of the LNA [13]. In turn, this causes the input return loss of the LNA to change according to the varying input impedance. Therefore, utilizing this topology as a variable-gain LNA may not guarantee good acceptable input return losses for all gain values. To alleviate this problem, the gain-varying part and the input-matching part of the LNA are segregated into two distinct stages.

The input-matching part becomes the first stage of the LNA as it is required to provide a suitable impedance match for input signals to the LNA. This input-matching stage utilizes the combination of complementary common-source current-reuse topology with active shunt feedback to sufficiently bring the input impedance down to 50 Ohm. The currents through both the complementary common-source current-reuse structure and the active shunt feedback source-follower structure in this stage of the LNA are fixed for steady input impedance.

The gain-varying stage of the LNA is separated from the input-matching stage by an inter-stage buffer in the form of a source-follower. This gain-varying stage also employs the complementary common-source current-reuse topology to maximize the gain of the LNA and minimize the noise figure with economical DC power consumption. To change the gain of the LNA, the current (hence DC power consumption) in the gain-varying stage is changed. This can be done by adjusting the gate-biasing voltages of both the NMOS and PMOS driver transistors in the complementary common-source current-reuse network of the gain-varying stage. This method of varying the gain is one of two methods utilized by [14] as gain-tuning knobs. In this work, this method is chosen over the other method in [14] because it is fairly straightforward to vary the gate-biasing voltages, for example, through an external microcontroller. This method also seems to be more practical and realistic in terms of physical realization of the IC, compared to the other method where many LNA cells of the same size are arranged together in parallel, thus will take up a significant amount of space in the IC.

The presence of an inter-stage buffer between the input-matching stage and the gain-varying stage of the LNA shields the input-matching stage from being affected by any current variation in the gain-varying stage. This is so

that the input impedance of the LNA may remain stable regardless of any change that occurs in the gain-varying stage. The block diagram in Fig. 1 illustrates the proposed structure of this variable-gain LNA.

In Fig. 1, the proposed variable-gain LNA consists of three distinct stages; the input-matching stage, the inter-stage buffer, and the gain-varying stage. The input-matching stage itself consists of two circuit structures, A and B. A is a complementary common-source current-reuse amplifier and B is a source-follower. The inter-stage buffer is made up of another source-follower, C. D is another complementary common-source current-reuse amplifier that represents the gain-varying stage of this LNA.

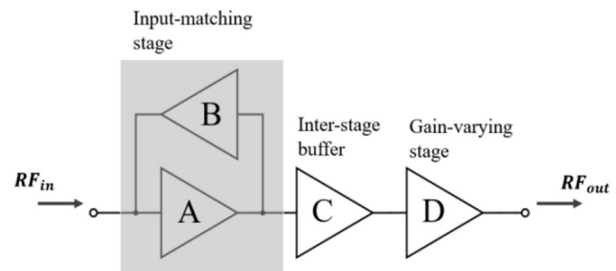


Fig. 1. Proposed structure of the variable-gain LNA in this work.

#### B. Input-Matching Stage

The main function of the input-matching stage is to provide an impedance match at the input of the LNA to obtain an acceptable input return loss. In addition to impedance match, this stage also provides initial gain to the LNA that will contribute to its overall gain. To carry out these functions, the input-matching stage consists of a complementary common-source current-reuse amplifier structure that drives the initial gain of the LNA and a source-follower network that acts as an active shunt feedback to present a suitable impedance at the input of the LNA for impedance match. The complementary common-source current-reuse structure is being utilized to obtain high gain and low noise figure with economical total DC power consumption. This is necessary and is a requirement for MedRadio biomedical devices. The source-follower shunt feedback network is being employed for input-matching purposes instead of the very common inductive-degeneration technique to avoid the use of bulky inductors. This is to attain a much smaller size of the IC, which is another requirement for MedRadio devices. Fig. 2 illustrates the schematic circuit diagram for the input-matching stage that comprises a complementary common-source current-reuse structure and a source-follower shunt feedback network.

In Fig. 2, the complementary common-source current-reuse structure is made up of NMOS transistor  $M_4$  and PMOS transistor  $M_3$  with  $M_3$  being stacked on top of  $M_4$  in the same DC current path. DC current  $I_{S2}$  flows from supply voltage  $V_{S2}$  through the source-drain channel of  $M_3$  and this same current is reused through  $M_4$ . Input AC signals are fed into the gates of  $M_3$  and  $M_4$  for amplification and the amplified output signals appear in-between the drains of both transistors. For both  $M_3$  and  $M_4$ , the bulk is tied to the source to eliminate body effects. The

source-follower shunt feedback network in Fig. 2 consists of NMOS transistors  $M_1$  and  $M_2$ , where  $M_1$  is the driving transistor and  $M_2$  functions as a current source. With this source-follower shunt feedback network, the input impedance of the LNA can be approximated by the impedance looking into the source terminal of  $M_1$ . Capacitors  $C_1$  to  $C_5$  are all needed to block DC currents from going into the AC signal transmission paths. Resistors  $R_1$  to  $R_3$  on the other hand, prevent AC signals from being shorted to ground.

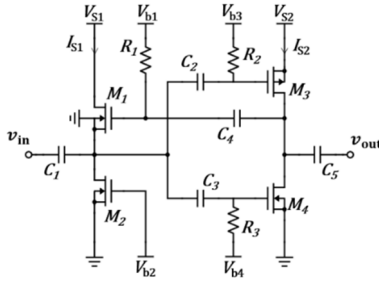


Fig. 2. Schematic circuit diagram of the input-matching stage.

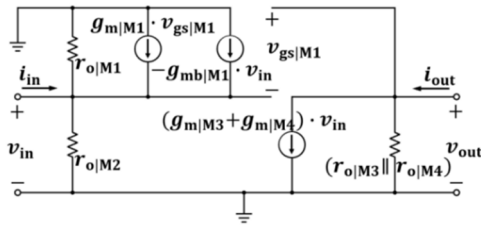


Fig. 3. Simplified small-signal equivalent circuit of the input-matching stage.

The simplified small-signal equivalent circuit of the input matching stage is depicted in Fig. 3 [18]. This small-signal equivalent circuit has been simplified by omitting capacitors  $C_1$  to  $C_5$  and resistors  $R_1$  to  $R_3$ . From Fig. 3, the low-frequency small-signal gain of the input-matching stage  $A_{v|IM}$  can be derived and simplified as:

$$A_{v|IM} = -\left(g_{m|M3} + g_{m|M4}\right) \frac{r_{o|M3} r_{o|M4}}{r_{o|M3} + r_{o|M4}} \quad (2)$$

where  $g_{m|M3}$  is the transconductance of  $M_3$ ,  $g_{m|M4}$  is the transconductance of  $M_4$ ,  $r_{o|M3}$  is the small-signal output resistance of  $M_3$  and  $r_{o|M4}$  is the small-signal output resistance of  $M_4$ . Equation (2) essentially indicates that the low-frequency small-signal gain of this input-matching stage can be increased with greater values for  $M_3$  and  $M_4$  transconductances and small-signal output resistances. This gain equation, however, only applies to low frequencies. As frequency increases, the effects of parasitic capacitances of the MOS transistors are becoming more prominent and thus may significantly affect the gain. Also from Fig. 3, the low-frequency small-signal input resistance of the input-matching stage  $r_{in|IM}$  can be derived as:

$$r_{in|IM} = \frac{1}{\frac{1}{r_{o|M1}} + \frac{1}{r_{o|M2}} + g_{mb|M1} + g_{m|M1} (1 - A_{v|IM})} \quad (3)$$

where  $r_{o|M1}$  and  $r_{o|M2}$  are the small-signal output resistances of  $M_1$  and  $M_2$ , respectively,  $g_{m|M1}$  is the transconductance of  $M_1$ ,  $g_{mb|M1}$  is the body transconductance of  $M_1$ , and  $A_{v|IM}$  is the low-frequency small-signal gain of the input-matching stage.  $r_{o|M1}$  and  $r_{o|M2}$  can be approximated to be very large since  $M_1$  and  $M_2$  are biased in the saturation region. Hence, (3) can be simplified and approximated to:

$$r_{in|IM} \approx \frac{1}{g_{mb|M1} + g_{m|M1} (1 - A_{v|IM})} \quad (4)$$

This simplified expression shows that the low-frequency small-signal input resistance is determined by the low-frequency small-signal gain of the input-matching stage and also by the transconductance and body transconductance of the driving transistor of the source-follower shunt feedback network, which is  $M_1$ . The noise factor of the input-matching stage  $F_{IM}$  can be derived as [12]:

$$F_{IM} = 1 + \frac{(\gamma_{M3} g_{m|M3} + \gamma_{M4} g_{m|M4}) R_{out|IM}^2}{A_{v|IM}^2 R_S} + \frac{(\gamma_{M1} g_{m|M1} + \gamma_{M2} g_{m|M2}) R_{out|IM}^2}{R_S} \quad (5)$$

where  $\gamma_{M1}$ ,  $\gamma_{M2}$ ,  $\gamma_{M3}$ , and  $\gamma_{M4}$  are the thermal noise coefficients for  $M_1$ ,  $M_2$ ,  $M_3$  and  $M_4$ , respectively,  $g_{m|M1}$ ,  $g_{m|M2}$ ,  $g_{m|M3}$  and  $g_{m|M4}$  are the transconductances of  $M_1$ ,  $M_2$ ,  $M_3$  and  $M_4$ , respectively,  $R_S$  is the source resistance,  $R_{in|IM}$  is the input resistance of the input-matching stage,  $R_{out|IM}$  is the output resistance of the input-matching stage and  $A_{v|IM}$  is the low-frequency small-signal gain of the input-matching stage. Since  $A_{v|IM}$  is part of the denominator in the second term of this expression, it implies that increasing the gain of the input-matching stage may improve its overall noise figure.

### C. Inter-Stage Buffer

The inter-stage buffer separates the input-matching stage from the gain-varying stage of the LNA. This separation is important to maintain a more or less consistent gain at the output of the input-matching stage regardless of any change that occurs in the gain-varying stage. With consistent gain, the input impedance generated by the input-matching stage will remain almost the same and unaffected. Thus, the input return loss will also be more or less unchanged. Maintaining a consistent gain at the output of this stage is a problem if the output of this stage is connected directly to the gain-varying stage. This is because the gain-varying stage will be subjected to changes in gate potential and drain-source current of its driving transistors. These changes, in turn, will subsequently affect the physical properties of the driving transistors, in particular, the gate-source and gate-drain capacitances. With changes in these capacitances, the higher frequency gain at the output of the input-matching stage will also change and this will significantly disrupt the consistency of input impedance (at the MedRadio band) generated by the input-matching stage. This whole thing can be prevented by having an inter-stage buffer that isolates the input-matching stage from the gain-varying stage. This inter-stage buffer employs a source-follower

structure. With this source-follower structure, the amplified signal that goes through the buffer from the input-matching stage is preserved as much as possible as if the signal at the buffer's output comes directly from the input-matching stage. This buffered signal is then channeled into the gain-varying stage for further amplification according to the desired LNA gain. Fig. 4 illustrates the schematic circuit diagram for this inter-stage buffer that is essentially made up of a source-follower structure.

The source-follower structure in Fig. 4 comprises NMOS transistors  $M_5$  and  $M_6$ .  $M_5$  functions as the driving transistor whilst  $M_6$  acts as the current source at the source of  $M_5$ . Resistor  $R_4$  prevents input AC signals from being grounded. The gate of  $M_5$  receives amplified AC signals from the input-matching stage and the buffered signals are passed on to the gain-varying stage via the source terminal of  $M_5$ . Fig. 5 illustrates the corresponding small-signal equivalent circuit for this inter-stage buffer with  $R_4$  omitted [18]. From here, the low-frequency small-signal gain of the inter-stage buffer can be approximated as:

$$A_{v|ISB} = \frac{g_{m|M5}}{g_{m|M5} + g_{mb|M5}} \quad (6)$$

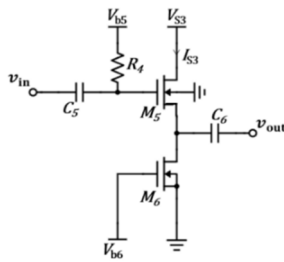


Fig. 4. Schematic circuit diagram of the inter-stage buffer.

where  $g_{m|M5}$  is the transconductance of  $M_5$  and  $g_{mb|M5}$  is the body transconductance of  $M_5$ . Just like the gain equation for a typical source-follower, Eq. (6) shows that the gain of the inter-stage buffer approaches unity as  $g_{m|M5}$  becomes larger.

The noise factor of the inter-stage buffer  $F_{ISB}$  can be derived and simplified as [12]:

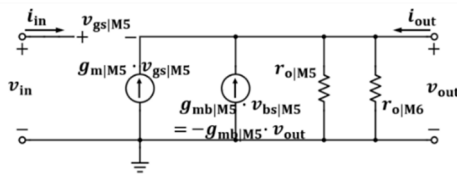


Fig. 5. Small-signal equivalent circuit for the inter-stage buffer.

$$F_{ISB} = 1 + \frac{(\gamma_{M5}g_{m|M5} + \gamma_{M6}g_{m|M6})R_{out|ISB}^2}{A_{v|ISB}^2 R_{out|ISB}} \quad (7)$$

where  $\gamma_{M5}$  and  $\gamma_{M6}$  are the thermal noise coefficients for  $M_5$  and  $M_6$ , respectively,  $g_{m|M5}$  and  $g_{m|M6}$  are transconductances of  $M_5$  and  $M_6$ , respectively,  $R_{out|IM}$  is the output resistance of the input-matching stage,  $R_{out|ISB}$  is the output resistance of the inter-stage buffer and  $A_{v|ISB}$  is the low-frequency small-signal gain of the inter-stage buffer. This expression indicates that the overall noise figure will

become higher if the inter-stage buffer gain becomes much less than unity. It therefore emphasizes the need to have a sufficiently high value of  $g_{m|M5}$  to obtain a gain that is very close to unity as given by Eq. (6).

#### D. Gain-Varying Stage

The function of the gain-varying stage is to enhance the initial gain provided by the input-matching stage to a greater gain value determined by the biasing of the NMOS and PMOS transistors of this stage. The amount of gain needed by the LNA very much depends on the strength of the input signal level to the LNA. If the input signal level is considerably high, the gain of the MedRadio LNA can be relaxed, hence lower DC power consumption with lower gain is acceptable. On the other hand, if the input signal is very weak, the gain needs to be further enhanced to amplify the weak input signal adequately. The DC power consumption must therefore be increased.

Fig. 6 depicts the schematic circuit diagram of the gain-varying stage. This gain-varying stage is made up of NMOS transistor  $M_8$  and PMOS transistor  $M_7$  as driver transistors in a complementary common-source current-reuse amplifier topology similar to that in the input-matching stage. The gate-biasing voltages  $V_{b7}$  and  $V_{b8}$  are to be adjusted to vary the gain of the LNA. This voltage adjustment can be done externally through a microcontroller. The resulting DC current  $I_{S4}$  flows from supply voltage  $V_{S4}$  through the source-drain channel of  $M_7$  and the drain-source channel of  $M_8$ . As the input AC signal from the inter-stage buffer goes into the gates of  $M_7$  and  $M_8$ , this signal is amplified, and the output signal appears in between the drains of both transistors. Just like  $M_3$  and  $M_4$  in the input-matching stage, the bulk is tied to the source for both  $M_7$  and  $M_8$  to eliminate body effects. Capacitors  $C_6$  and  $C_7$  are needed to block DC currents from going into the AC signal transmission paths. Resistors  $R_5$  and  $R_6$  meanwhile, prevent the input signal from being grounded. The corresponding small-signal equivalent circuit of the gain-varying stage is illustrated in Fig. 7 [18]. This small-signal equivalent circuit has been simplified by omitting capacitors  $C_6$  and  $C_7$ , and resistors  $R_5$  and  $R_6$ .

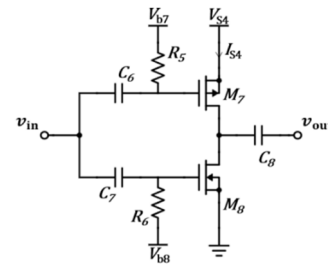


Fig. 6. Schematic circuit diagram of the gain-varying stage.

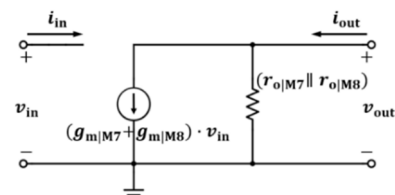


Fig. 7. Simplified small-signal equivalent circuit of the gain-varying stage.

From Fig. 7, the low-frequency small-signal gain of the gain-varying stage can be derived and simplified as:

$$A_{v|GV} = -\left(g_{m|M7} + g_{m|M8}\right) \frac{r_{o|M7} r_{o|M8}}{r_{o|M7} + r_{o|M8}} \quad (8)$$

where  $g_{m|M7}$  is the transconductance of  $M_7$ ,  $g_{m|M8}$  is the transconductance of  $M_8$ ,  $r_{o|M7}$  is the small-signal output resistance of  $M_7$  and  $r_{o|M8}$  is the small-signal output resistance of  $M_8$ . Similar to (2) for the input-matching stage, (8) for the gain-varying stage also indicates that the low-frequency small-signal gain will become higher with greater values for the transconductances and the small-signal output resistances of both  $M_7$  and  $M_8$ . As frequency increases, the parasitic capacitances of the MOS transistors are starting to exert more prominent effects and thus may degrade the gain in the MedRadio frequency band. The noise factor of the gain-varying stage  $F_{GV}$  can be derived as [12]:

$$F_{GV} = 1 + \frac{(\gamma_{M7} g_{m|M7} + \gamma_{M8} g_{m|M8}) R_{out|GV}^2}{A_{v|GV}^2 R_{out|GV}} \quad (9)$$

where  $\gamma_{M7}$  and  $\gamma_{M8}$  are the thermal noise coefficients for  $M_7$  and  $M_8$ , respectively,  $g_{m|M7}$  and  $g_{m|M8}$  are transconductances of  $M_7$  and  $M_8$ , respectively,  $R_{out|ISB}$  is the output resistance of the inter-stage buffer,  $R_{out|GV}$  is the output resistance of the gain-varying stage and  $A_{v|GV}$  is the low-frequency small-signal gain of the gain-varying stage. Similar to (5) for the input-matching stage, (9) for the gain-varying stage also implies that increasing the gain of the gain-varying stage may improve its overall noise figure.

### E. Full Circuit

The full circuit of this variable-gain LNA is obtained by cascading all three components of it; the input-matching stage, the inter-stage buffer, and the gain-varying stage. The full schematic circuit of this variable-gain MedRadio LNA is depicted in Fig. 8. Based on the gain equations for the input-matching stage, the inter-stage buffer, and the gain-varying stage mentioned previously, the gain of the variable-gain MedRadio LNA can be expressed as [12]:

$$A_{v|VGLNA} = A_{v|IM} A_{v|ISB} A_{v|GV} \quad (10)$$

By using Friis Formula, the simplified noise factor of the variable-gain MedRadio LNA can be deduced as [12]:

$$F_{VGLNA} = F_{IM} + \frac{F_{ISB} - 1}{A_{v|IM}} + \frac{F_{GV} - 1}{A_{v|IM} A_{v|ISB}} \quad (11)$$

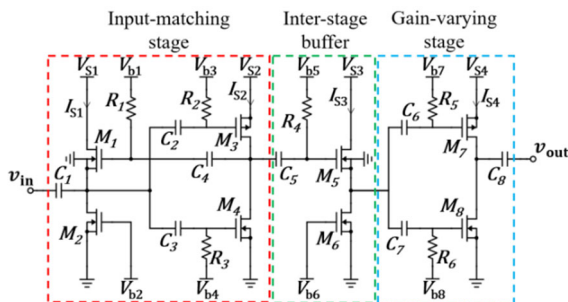


Fig. 8. Full schematic circuit of variable-gain MedRadio LNA.

TABLE I: TRANSISTOR GATE DIMENSIONS

Transistor	Gate length ( $\mu\text{m}$ )	Total gate width ( $\mu\text{m}$ )
$M_1$	0.18	29.67
$M_2$	0.18	6.01
$M_3$	0.18	136.5
$M_4$	0.18	139.6
$M_5$	0.18	33.76
$M_6$	0.18	60.64
$M_7$	0.18	207.84
$M_8$	0.18	109.48

Table I summarizes the chosen gate dimensions for all the transistors in Fig. 8. The chosen values for all capacitors and resistors are 10 pF and 500 k $\Omega$ , respectively. For the capacitors, the selected value of 10 pF is deemed acceptable to sufficiently allow MedRadio signals to travel all the way through the transmission path yet at the same time not acquire too much space to cause the physical size of the LNA to be too bulky. The same goes for the resistors where the resistance value is maximized to 500 k $\Omega$  to prevent AC signals in the transmission path from being grounded but at the same time not causing the resistors to be too large in physical size.

Table II lists the operating voltage levels for all the voltage points in Fig. 8.  $V_{b7}$  and  $V_{b8}$  are variable voltage points that determine the overall gain and total DC power consumption of this LNA. Hence, these two voltage points are the “knobs” for gain adjustments. Through DC simulations, the values of  $V_{b7}$  and  $V_{b8}$  that may give out overall LNA gain ranging from approximately 10 dB to 30 dB have been identified. The approximate values of current and DC power consumption for all stages of the LNA are tabulated in Table III.

TABLE II: OPERATING VOLTAGE LEVELS FOR ALL VOLTAGE POINTS

Voltage point	Voltage (V)
$V_{S1}$	0.6
$V_{S2}$	0.6
$V_{S3}$	0.6
$V_{S4}$	1.8
$V_{b1}$	0.85
$V_{b2}$	0.6
$V_{b3}$	0
$V_{b4}$	0.5
$V_{b5}$	0.9
$V_{b6}$	0.5
$V_{b7}$	1.25 $\cap$ 1.31 (for $V_{b8} = 0.5$ V) 1.30 $\cap$ 1.39 (for $V_{b8} = 0.45$ V) 1.38 $\cap$ 1.45 (for $V_{b8} = 0.4$ V)
$V_{b8}$	0.4, 0.45, 0.5

TABLE III: CURRENTS AND DC POWER CONSUMPTIONS FOR ALL STAGES

Stage	Current (mA)	DC power consumption (mW)
Source-follower of input-matching stage	$\sim 0.07$	$\sim 0.042$
Complementary common-source current-reuse amplifier of input-matching stage	$\sim 0.5$	$\sim 0.3$
Inter-stage buffer	$\sim 0.2$	$\sim 0.12$
Gain-varying stage	$\sim 0.02$ to $\sim 0.5$	$\sim 0.035$ to $\sim 0.9$

### F. Layout Design 0.18 $\mu\text{m}$

In this work, Silterra’s CMOS technology is employed. The physical layout for this variable-gain LNA is

illustrated in Fig. 9. The total die area ( $a_{\text{die}}$ ) occupied by this LNA is approximately  $0.08 \text{ mm}^2$ .

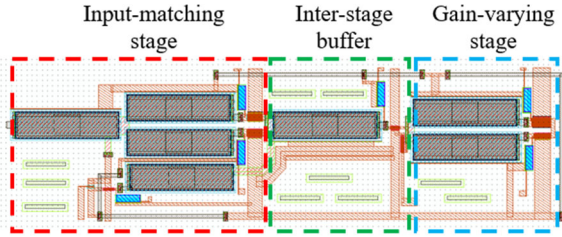


Fig. 9. IC layout of variable-gain MedRadio LNA in this work.

#### IV. POST-LAYOUT SIMULATION RESULTS AND DISCUSSIONS

##### A. General Performance

Using the values in Table II, post-layout simulations with a source-follower output buffer were performed for gain ( $A_v$ ), input return loss ( $RL_{\text{in}}$ ), noise figure (NF), input-referred 1 dB compression point ( $IP_{1\text{dB}}$ ) and input third-order intercept point ( $IIP_3$ ) at MedRadio frequencies. The plots for all these parameters and also for total DC power

consumption ( $P_{\text{DC}}$ ) against  $V_{b7}$  are illustrated in Fig. 10 (a)–Fig. 10 (f). Table IV summarizes the simulated performance at the maximum and minimum gain values.

Fig. 10 (a) and Table IV show a wide variation in the gain of the LNA from a maximum of 29.1 dB at 1.34 mW DC power consumption to a minimum of 11.2 dB at 0.49 mW DC power consumption. This clearly shows a trade-off between gain and DC power consumption, where more DC power must be dissipated when a higher gain is required. In this case, more than 1 mW of DC power is needed to increase the gain to nearly 30 dB. Conversely, only less than 0.5 mW of DC power needs to be consumed when the gain can be relaxed to as low as 11 dB. The difference in gain between high and low DC power consumption is due to the difference in current in the complementary common-source current-reuse structure of the gain-varying stage, which is caused by varying biasing voltages  $V_{b7}$  and  $V_{b8}$ . As the current is varied at the gain-varying stage, the total transconductance of the stage also changes accordingly. Hence, this change in total transconductance results in the variation of the gain as indicated by (8).

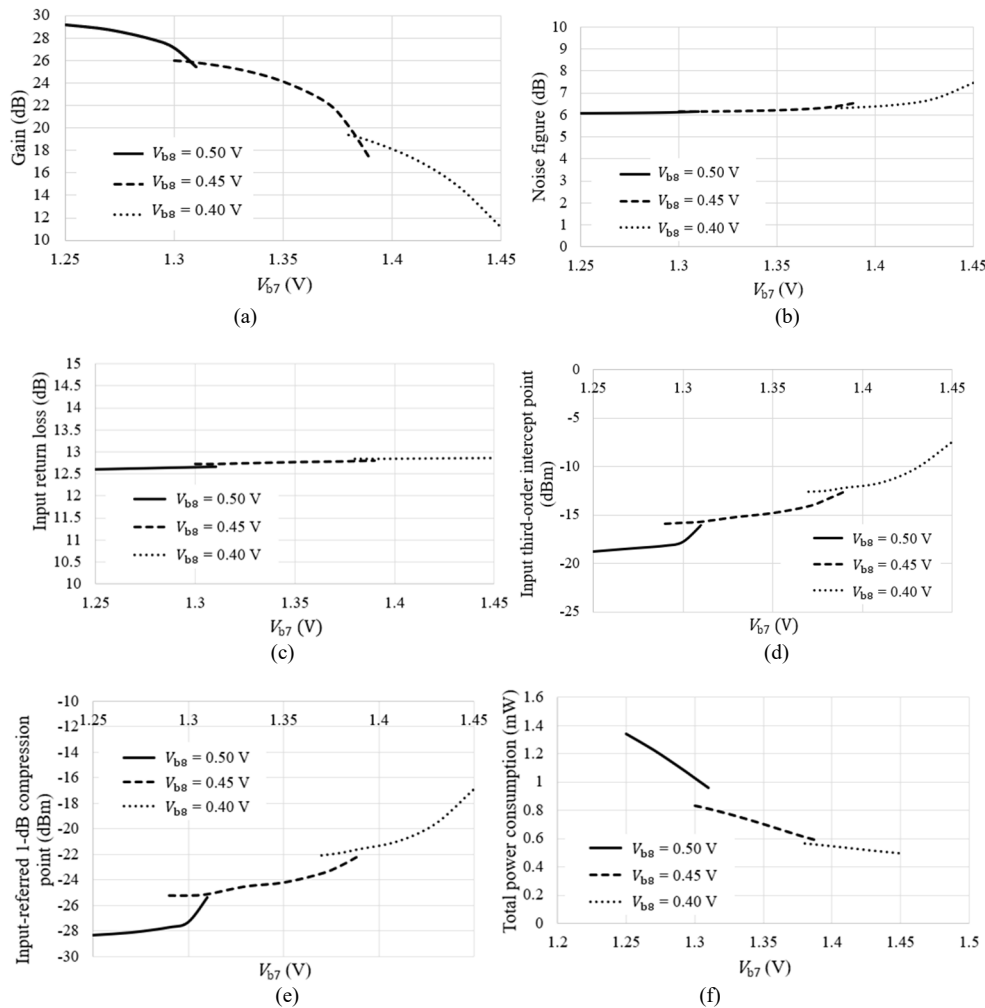


Fig. 10. Plot of (a) gain versus  $V_{b7}$  from post-layout simulations of the variable-gain MedRadio LNA in this work; (b) noise figure versus  $V_{b7}$  from post-layout simulations of the variable-gain MedRadio LNA in this work; (c) input return loss versus  $V_{b7}$  from post-layout simulations of the variable-gain MedRadio LNA in this work; (d) input third-order intercept point versus  $V_{b7}$  from post-layout simulations of the variable-gain MedRadio LNA in this work; (e) input-referred 1-dB compression point versus  $V_{b7}$  from post-layout simulations of the variable-gain MedRadio LNA in this work; (f) total power consumption versus  $V_{b7}$  from post-layout simulations of the variable-gain MedRadio LNA in this work.

TABLE IV: POST-LAYOUT SIMULATION RESULTS AT MAXIMUM AND MINIMUM GAIN VALUES

Parameter	Maximum gain	Minimum gain
Operating frequency (MHz)	401 - 406	401 - 406
$A_v$ (dB)	29.1	11.2
$RL_{in}$ (dB)	12.6	12.9
NF (dB)	6.1	7.5
$IP_{1dB}$ (dBm)	-28.3	-16.9
$IIP_3$ (dBm)	-18.8	-7.5
Total DC power consumption (mW)	1.34	0.49

Such wide variation of the gain is not exhibited by the noise figure however, where the noise figure only differs by just 1.4 dB from 6.1 dB at maximum gain to 7.5 dB at minimum gain as shown in Fig. 10 (b) and Table IV. Hence, increasing the DC power consumption from 0.49 mW (at minimum gain) to 1.34 mW (at maximum gain) only improves the noise figure by less than 2 dB. This small variation of noise figure can be explained by the fact that gain is varied in the gain-varying stage which is the third stage of the LNA. Eq. (11) indicates that the noise contribution from the gain-varying stage is not as significant as those from the two earlier stages, namely the input-matching stage and the inter-stage buffer. Hence, changes in the noise of the gain-varying stage may not greatly affect the total noise figure of the LNA.

From Fig. 10 (c) and Table IV, the variation in input return loss from maximum gain to minimum gain is also shown to be very small at only 0.3 dB. This is desirable since the gain of the LNA can be adjusted and varied without having to worry about the input impedance match. This very little variation of input return loss can be attributed to the presence of the inter-stage buffer between the input-matching stage and the gain-varying stage. The inter-stage buffer shields the input-matching stage from being affected by any current variation in the gain-varying stage. This shielding results in a consistent gain at the output of the input-matching stage regardless of any change that occurs in the gain-varying stage due to changes made to  $V_{b7}$  and  $V_{b8}$ . With consistent gain, the input impedance generated by the input-matching stage will remain almost the same and unaffected, thus, resulting in a very stable input return loss.

In Fig. 10 (d) and Fig. 10 (e), the variations in  $IIP_3$  and  $IP_{1dB}$  look to be almost identical since these two parameters are closely related as implied by (1). The variations of these parameters are shown to be almost in opposite correlation with the variation in gain depicted in Fig. 10 (a). This is consistent with the general fact that the linearity of an amplifier improves as the gain decreases, and vice versa. However, the variations in both  $IIP_3$  and  $IP_{1dB}$  shown in Fig. 10 (d)–(e) are just around 11 dB between the maximum gain of 29.1 dB at 1.34 mW DC power consumption, and the minimum gain of 11.2 dB at 0.49 mW DC power consumption. Since MedRadio signals are typically very low and weak RF signals, with an estimated maximum received power of just around -30 dBm at the receiver input, the linearity performance of this proposed LNA should not be much of a concern as long as it does not start to saturate below -30 dBm of input power level.

Fig. 10 (f) illustrates how the total power consumption of the LNA varies with biasing voltage  $V_{b7}$  using 3

different values of biasing voltage  $V_{b8}$ . It shows that the total power consumption of the LNA can be varied from as low as 0.49 mW (with  $V_{b7}$  of 1.45 V and  $V_{b8}$  of 0.40 V) to as high as 1.34 mW (with  $V_{b7}$  of 1.25 V and  $V_{b8}$  of 0.50 V). This range of power consumption results in a wide variation in the gain of the LNA from a minimum of 11.2 dB at 0.49 mW power consumption to a maximum of 29.1 dB at 1.34 mW power consumption as shown earlier by Fig. 10 (a). The difference in power consumption between maximum and minimum LNA gain is brought about by the difference in current in the complementary common-source current-reuse structure of the gain-varying stage, which is caused by varying biasing voltages  $V_{b7}$  and  $V_{b8}$ .

### B. Comparison with Previous Works

To the best of the authors' knowledge, there has been no published work on stand-alone MedRadio LNA since [13] in 2020. Hence, MedRadio band performance comparisons are made with some of the most recent works on wideband LNA that are suitable for MedRadio applications. These are presented in Table V. The Figure of Merit (FOM) in Table V is defined as:

$$FOM = \frac{A_v \times RL_{in}}{P_{DC}^2 \times NF \times a_{die}^2} \quad (12)$$

where  $A_v$ ,  $RL_{in}$  and NF are in magnitudes,  $P_{DC}$  is in W, and  $a_{die}$  is in  $m^2$ .

Table V directly shows the main advantage of the proposed variable-gain LNA in this work as compared to other recent LNAs in the table, which is its ability to vary its gain from 29.1 dB at 1.34 mW power consumption to 11.2 dB at 0.49 mW power consumption. This may enable the proposed LNA to perform with better efficiency in terms of power and performance. That is, when the input signal level is sufficiently very high, the DC power consumption of the LNA can be reduced for power saving by lowering the gain. Conversely, if the input signal level is extremely low, the LNA can be operated at a much higher gain albeit with greater DC power consumption.

The high maximum gain of 29.1 dB for the proposed LNA is due to the sum of gains from the input-matching stage and the gain-varying stage. With both stages employing the complementary common-source current-reuse amplifier structure, and the presence of an inter-stage buffer to assist this gain summation, a very high maximum overall gain of the proposed LNA can be expected. For previous works in Table V, these are also multi-stage LNAs utilizing combinations of common-source and common-gate circuits with or without current-reuse. However, the absence of a buffer between the amplification stages in these previous works significantly affects the output impedance of the preceding amplification stage hence reducing its gain at higher frequencies.

For this proposed LNA, the noise figure ranges from 6.1 dB to 7.5 dB across the gain range, and this is relatively high compared to the noise figures from other recent works in Table V. This can be explained by the fact that the proposed variable-gain LNA in this work consists of three distinct stages that provide their noise contributions to the



total noise figure of the LNA. In other recent LNAs in Table V, some noise figure improvement measures such as noise-cancelling circuit techniques are employed. These techniques, however, consume a significant amount of

additional DC power. Hence, this helps to explain the relatively high LNA DC power consumption in these previous works.

TABLE V: MEDRADIO BAND PERFORMANCE COMPARISON WITH SOME RECENT WORKS ON WIDEBAND LNA

Para-meter	This work*		[19]	[20]	[21]	[22]	[23]	[24]
	Max. gain	Min. gain						
CMOS tech. ( $\mu\text{m}$ )	0.18	0.18	0.09	0.13	0.18	0.028	0.028	0.065
$P_{\text{DC}}$ (mW)	1.34	0.49	1.2	3.24	3	4.1	4.5	6.6
$A_v$ (dB)	29.1	11.2	21	14	19	18.5	15.2	17.5
$RL_{\text{in}}$ (dB)	12.6	12.9	20	12	15	16.2	16	18
NF (dB)	6.1	7.5	3.5	4	3.8	2.9	2.8	2.1
$IP_{1\text{dB}}$ (dBm)	-28.3	-16.9	-20	N/A	-15.5	N/A	N/A	N/A
$IIP_3$ (dBm)	-18.8	-7.5	-7.1	2	-8	2	-4.6	8
$a_{\text{die}}$ ( $\text{mm}^2$ )	0.08	0.08	0.075	0.1	0.18	0.022	0.03	0.062
FOM	$2.60 \times 10^{21}$	$1.86 \times 10^{21}$	$6.19 \times 10^{21}$	$7.72 \times 10^{19}$	$7.16 \times 10^{19}$	$3.42 \times 10^{21}$	$1.05 \times 10^{21}$	$2.19 \times 10^{20}$

\* All post-layout simulation data

The input return loss of the proposed LNA is more than 2 dB above the usual return loss requirement of 10 dB for most RF systems. However, this is considerably low compared to those of previous works in Table V except [20]. This is due to the use of source-follower shunt feedback network for input-matching purposes in the proposed LNA. With the source-follower shunt feedback network, the low-frequency approximation for the small-signal input resistance of the input-matching stage is given by (4). However, at MedRadio frequencies, the effects of parasitic capacitances of the MOS transistors are getting more prominent. This causes the small-signal input resistance expression in (4) to be less accurate at MedRadio frequencies, hence affecting the input return loss obtained through simulation. In all the previous works in Table V, a common-gate wideband input-matching technique is employed. This technique is much more effective for wideband input-matching but at the expense of considerably high DC power consumption.

For this proposed LNA, the linearity parameters  $IIP_3$  and  $IP_{1\text{dB}}$  at maximum gain are relatively low compared to the  $IIP_3$  and  $IP_{1\text{dB}}$  values for other recent works in Table V. This is consistent with the high maximum gain of the proposed LNA compared to those of previous works in Table V, and the fact that linearity degrades as gain becomes higher. In addition, some of the previous works in Table V also employ distortion-cancelling techniques that may further help to improve the LNA's linearity. However, this linearity improvement technique also consumes additional DC power that may contribute to higher overall DC power consumption. As stated previously, the linearity performance of this proposed MedRadio LNA should not be much of a concern due to the very low and weak power levels of MedRadio signals.

Although the proposed LNA consists of three distinct stages, the total die area is just  $0.08 \text{ mm}^2$ , which is relatively very small for a MedRadio LNA utilizing  $0.18 \mu\text{m}$  CMOS technology. This very small total die area is mostly due to the inductorless design topology utilized in this work. Some of the previous works in Table V, such as [19, 22–24] are employing CMOS technologies that are finer than  $0.1 \mu\text{m}$ . With these very fine CMOS

technologies, these LNAs can acquire much smaller die sizes compared to those of the proposed LNA.

For overall performance, the FOMs for both the maximum and minimum gain values of the proposed LNA are higher than that of [20, 21, 23] and [24] as given in Table V. The considerably good FOMs for both the maximum and minimum gain values are mostly due to the low DC power consumption of the proposed LNA.

### C. Temperature Variation

For both the maximum and minimum gain values, post-layout simulations were also performed at lower and upper ends of room temperature range. This is to study the effect of temperature variation on the performance of the proposed MedRadio LNA in this work. The temperature variation studied is only around the room temperature range and does not include extreme temperatures such as less than  $0 \text{ }^\circ\text{C}$  or greater than  $50 \text{ }^\circ\text{C}$ . This is based on the assumption that medical treatments utilizing the proposed LNA (as a component of a MedRadio biomedical device) are only carried out on patients at room temperature. In this work, the lower and upper ends of room temperature range are defined at  $20 \text{ }^\circ\text{C}$  and  $30 \text{ }^\circ\text{C}$ , respectively. The performances of the LNA at the maximum and minimum gain values were chosen for this study since these two conditions consume the most and the least DC power. The simulation results are summarized in Table VI.

 TABLE VI: POST-LAYOUT SIMULATION RESULTS AT LOWER ( $20 \text{ }^\circ\text{C}$ ) AND UPPER ( $30 \text{ }^\circ\text{C}$ ) ENDS OF ROOM TEMPERATURE RANGE FOR MAXIMUM AND MINIMUM GAIN VALUES

Parameter	Maximum gain			Minimum gain		
	$20 \text{ }^\circ\text{C}$	Nom.	$30 \text{ }^\circ\text{C}$	$20 \text{ }^\circ\text{C}$	Nom.	$30 \text{ }^\circ\text{C}$
$P_{\text{DC}}$ (mW)	1.22	1.34	1.39	0.45	0.49	0.51
$A_v$ (dB)	28.9	29.1	29.4	10.3	11.2	11.6
$RL_{\text{in}}$ (dB)	11.0	12.6	13.4	11.2	12.9	13.7
NF (dB)	6.1	6.1	6.1	7.6	7.5	7.4
$IP_{1\text{dB}}$ (dBm)	-28.9	-28.3	-28	-17.8	-16.9	-16.6
$IIP_3$ (dBm)	-19.4	-18.8	-18.5	-8.4	-7.5	-7.2

Nominal (nom.) temperature used in this work is  $27 \text{ }^\circ\text{C}$ .

In Table VI, across the room temperature range from  $20 \text{ }^\circ\text{C}$  to  $30 \text{ }^\circ\text{C}$ , the total DC power consumption slightly increases for both maximum and minimum gain values. This is due to the increase in total current as the

temperature is raised. The increase in total DC power consumption for maximum gain is greater than that for minimum gain since there is a much larger current in the gain-varying stage of the LNA at maximum gain. As the temperature is raised from 20°C to 30°C, the gain also increases slightly due to the increase in current. This increase in gain however, does not exceed 2 dB for both maximum and minimum gain values. Other parameters such as input return loss,  $IP_{1dB}$  and  $IIP_3$  also exhibit some changes albeit very slightly. Overall, all test parameters of this proposed LNA are not significantly affected by variation across the room temperature range.

D. Monte Carlo Analysis

Post-layout Monte Carlo simulations were performed to understand the effect of IC process variations and mismatches on large-sample performance of the proposed LNA, and to show how the variable-gain LNA in this work can be used to mitigate the effect. Fig. 11 presents the gain histogram plot from post-layout Monte Carlo simulation of the proposed variable-gain MedRadio LNA with  $V_{b8}=0.45$  V and  $V_{b7}=1.35$  V. The number of iterations is 1000. In Fig. 11, the yield for gain of greater than 23 dB is 60.0%. This yield percentage can actually be improved by slightly reducing  $V_{b7}$ .

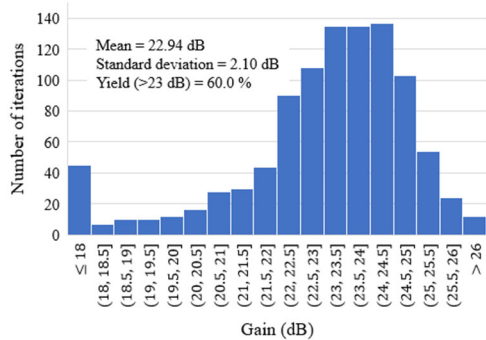


Fig. 11. Histogram plot of gain distribution with  $V_{b8} = 0.45$  V and  $V_{b7} = 1.35$  V from post-layout Monte Carlo simulation of the variable-gain MedRadio LNA in this work.

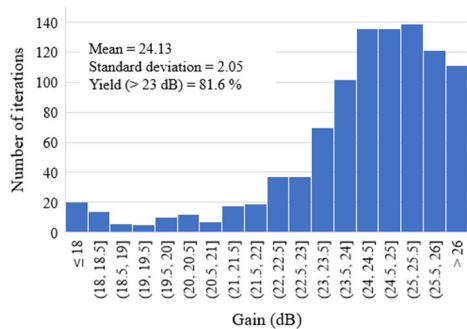


Fig. 12. Histogram plot of gain distribution with  $V_{b8} = 0.45$  V and  $V_{b7} = 1.33$  V from post-layout Monte Carlo simulation of the variable-gain MedRadio LNA in this work.

The histogram plot for gain when  $V_{b7}$  is reduced to 1.33 V is shown in Fig. 12. In Fig. 12, the yield for gain of greater than 23 dB is shown to have improved to 81.6 %. This small reduction of  $V_{b7}$  to increase the gain (thus improving the yield) is consistent with the gain versus  $V_{b7}$  plot in Fig. 10 (a). However, this increases the total DC

power consumption of the proposed LNA as the current in the gain-varying stage is increased.

V. CONCLUSIONS

A variable-gain 0.18  $\mu$ m CMOS LNA for MedRadio applications has been designed and verified through simulations in Cadence IC5 with Silterra’s C18G CMOS technology Process Design Kit. This LNA is capable of varying its gain from just above 10 dB to nearly 30 dB. With this capability, the LNA may perform with better power-performance efficiency. This proposed variable-gain LNA consists of an input-matching stage, an inter-stage buffer and a gain-varying stage. The main function of the input-matching stage is to provide impedance match for optimum input signal power transfer. It also provides an initial gain that will contribute to the overall LNA gain. The inter-stage buffer isolates the input-matching stage from the gain-varying stage. The function of the gain-varying stage is to enhance the initial gain provided by the input-matching stage to the overall gain value which is determined by the variable biasing of the driving transistors of the gain-varying stage.

On simulations, this proposed variable-gain LNA exhibits a wide-ranging gain from a maximum of 29.1 dB at 1.34 mW DC power consumption to a minimum of 11.2 dB at 0.49 mW DC power consumption. The advantage of this proposed variable-gain MedRadio LNA in comparison to other previous works on MedRadio LNA is its ability to vary its gain. This allows the LNA to perform with better power-performance efficiency, where the gain can be reduced for power saving if the input signal level is sufficiently very high, and the gain can be raised if the input signal level is extremely low. This ability may also help to counteract and mitigate the effect of process variations and mismatches in the LNA integrated circuit for yield improvement. The total die area occupied by the LNA in this work is just 0.08 mm<sup>2</sup> which is relatively very small for a MedRadio LNA utilizing 0.18  $\mu$ m CMOS technology.

CONFLICT OF INTEREST

The authors declare no conflict of interest.

AUTHOR CONTRIBUTIONS

All authors conducted the research; the first author carried out the design and simulation work, and all authors analyzed the simulation data. The first author wrote the paper. All authors had approved the final version.

FUNDING

This work was supported by Ministry of Higher Education, Malaysia for Fundamental Research Grant Scheme with Project Code: FRGS/1/2019/TK04/USM/02/3.

ACKNOWLEDGMENT

The authors would like to thank the Collaborative Microelectronic Design Excellence Center (CEDEC) of

Universiti Sains Malaysia for support on Cadence IC5 software and Silterra Process Design Kit.

REFERENCES

[1] T. Copani, S. Min, S. Shashidharan *et al.*, "A CMOS low-power transceiver with reconfigurable antenna interface for medical implant applications," *IEEE Trans. Microw. Theory Tech.*, vol. 59, no. 5, pp. 1369–1378, May 2011.

[2] A. Marzuki, M. A. Mubin, C. H. Wong, and M. T. Mustafa, "Design of MedRadio RF mixer by utilizing subthreshold biasing and bleeding circuit techniques," in *Proc. 2021 ICCCE Conf.*, 2021, pp. 283–287.

[3] S. Singh and D. Prasad, "Wireless body area network (WBAN): A review of schemes and protocols," *Mater. Today: Proc.*, vol. 49, pp. 3488–3496, Jan. 2022.

[4] X. Hu, W. Yin, F. Du *et al.*, "Biomedical applications and challenges of in-body implantable antenna for implantable medical devices: A review," *AEU - Int. J. Electron. Commun.*, no. 174, pp. 155053–155068, Jan. 2024.

[5] H. K. Cha, M. K. Raja, X. Yuan, and M. Je, "A CMOS MedRadio receiver RF front-end with a complementary current-reuse LNA," *IEEE Trans. Microw. Theory Tech.*, vol. 59, no. 7, pp. 1846–1854, Jul. 2011.

[6] A. Rajaiyan and M. Saberi, "A highly-linear wideband differential low-noise amplifier using derivative superposition technique," in *Proc. 2022 ICEE Conf.*, 2022, pp. 480–484.

[7] G. Chang, S. Maity, B. Chatterjee, and S. Sen, "Design considerations of a sub-50  $\mu$ W receiver front-end for implantable devices in MedRadio band," in *Proc. 2018 VLSID Conf.*, 2018, pp. 329–334.

[8] G. Feng, L. Zheng, Y. Wang, and Q. Xue, "A 0.5-V 0.88-mW low noise amplifier with active and passive  $g_m$  enhancements in sub-6 GHz band," *IEEE Microw. Wirel. Compon. Lett.*, vol. 33, no. 8, pp. 1159–1162, Aug. 2023.

[9] H. L. J. Jeong, J. Kim, and D. S. Ha, "A reliable ultra low power merged LNA and mixer design for Medical Implant Communication Services," in *Proc. IEEE/NIH Life Sci. Syst. Appl. Work.*, Bethesda, 2011, pp. 51–54.

[10] H. Cruz, H. Y. Huang, S. Y. Lee, and C. H. Luo, "Analysis and design of a 1.3-mW current-reuse RF front-end for the MICS band," in *Proc. 2014 ISCAS Conf.*, 2014, pp. 1360–1363.

[11] A. Srivastava, N. Sankar, K. K. Rakesh, B. Chatterjee, D. Das, and M. S. Baghini, "Design and measurement techniques for a low noise amplifier in a receiver chain for MedRadio spectrum of 401-406 MHz frequency band," in *Proc. 2016 VDAT Conf.*, 2016, pp. 1–6.

[12] B. Razavi, *RF Microelectronics*, 2<sup>nd</sup> ed., Upper Saddle River, NJ, USA: Prentice Hall PTR, 1998, pp. 40–58.

[13] M. A. Mubin and A. Marzuki, "A low-noise amplifier utilizing current-reuse technique and active shunt feedback for MedRadio band applications," *Int. J. Electr. Electron. Eng. Telecommun.*, vol. 9, no. 5, pp. 306–316, Jan. 2020.

[14] G. Chang, S. Maity, B. Chatterjee, and S. Sen, "A MedRadio receiver front-end with wide energy-quality scalability through circuit and architecture-level reconfigurations," *IEEE J. Emerg. Sel.*, vol. 8, no. 3, pp. 369–378, Sep. 2018.

[15] J. Y. Hsieh and K. Y. Lin, "A 0.6-V low-power variable-gain LNA in 0.18- $\mu$ m CMOS Technology," *IEEE Trans. Circuits Syst. II: Express Br.*, vol. 67, no. 1, pp. 23–26, Jan. 2020.

[16] H. Khosravi, M. Shekhi, A. Bijari, and N. Kandalafi, "3.5-9 GHz ultra-wideband LNA with variable gain and noise cancellation for wireless communication," in *Proc. 2020 CCWC Conf.*, 2020, pp. 0396–0401.

[17] F. Soleymani, Y. Bastan, P. Amiri, and M. H. Maghami, "A 0.3–1.4 GHz inductorless CMOS variable gain LNA based on the inverter cell and self-forward-body-bias technique," *AEU - Int. J. Electron. Commun.*, vol. 113, pp. 152974–152982, Jan. 2020.

[18] P. R. Gray, P. J. Hurst, S. H. Lewis, and R. G. Meyer, *Analysis and Design of Analog Integrated Circuits*, 5<sup>th</sup> ed., New York, USA: John Wiley & Sons, Inc., 2010, pp. 178–196.

[19] K. W. Cheng, W. W. Chen, and S. D. Yang, "A low power sub-GHz wideband LNA employing current-reuse and device-reuse positive shunt-feedback technique," *IEEE Microw. Wirel. Compon. Lett.*, vol. 32, no. 12, pp. 1455–1458, Dec. 2022.

[20] D. Kim, S. Jang, J. Lee, and D. Im, "A broadband PVT-insensitive

all-nMOS noise-canceling balun-LNA for subgigahertz wireless communication applications," *IEEE Microw. Wirel. Compon. Lett.*, vol. 31, no. 2, pp. 165–168, Feb. 2021.

[21] S. Tiwari and J. Mukherjee, "An inductorless wideband  $g_m$ -boosted balun LNA with nMOS-pMOS configuration and capacitively coupled loads for sub-GHz IoT applications," *IEEE Trans. Circuits Syst. II Express Briefs*, vol. 68, no. 10, pp. 3204–3208, Oct. 2021.

[22] A. Bozorg and R. B. Staszewski, "A 20 MHz–2 GHz inductorless two-fold noise-canceling low-noise amplifier in 28-nm CMOS," *IEEE Trans. Circuits Syst. I Regul. Pap.*, vol. 69, no. 1, pp. 42–50, Jan. 2022.

[23] A. Bozorg and R. B. Staszewski, "A 0.02–4.5-GHz LN(T)A in 28-nm CMOS for 5G exploiting noise reduction and current reuse," *IEEE J. Solid-State Circuits*, vol. 56, no. 2, pp. 404–415, Feb. 2021.

[24] R. Zhou, S. Liu, J. Liu, Y. Liang, and Z. Zhu, "A 0.1–3.5-GHz inductorless noise-canceling CMOS LNA with IIP3 optimization technique," *IEEE Trans. Microw. Theory Tech.*, vol. 70, no. 6, pp. 3234–3243, Jun. 2022.

Copyright © 2024 by the authors. This is an open access article distributed under the Creative Commons Attribution License (CC BY-NC-ND 4.0), which permits use, distribution and reproduction in any medium, provided that the article is properly cited, the use is non-commercial and no modifications or adaptations are made.



**Mutanizam Abdul Mubin** obtained his B.Eng. (Hons.) degree in electronic engineering from the University of Leeds, U.K. in 2003, and his M.Sc. (by research) degree in integrated circuit design from Universiti Sains Malaysia in 2019. From December 2003 to July 2016, he worked as a R&D/NPI product development engineer at Broadcom Inc. (previously known as Avago Technologies, and previously as Semiconductor Products Group of Agilent Technologies) in Penang, Malaysia. He is now pursuing his Ph.D. degree on a full-time basis at Universiti Sains Malaysia in the field of integrated circuit design.



**Mohd Tafir Mustaffa** received his B.Eng. degree in electrical and electronic engineering from Universiti Sains Malaysia (USM), Penang in 2000. He was awarded a master's degree (M.Eng.Sc) in computer and microelectronic engineering from Victoria University, Australia in 2005 and officially completed his Ph.D. degree in electrical engineering specializing in Radio Frequency Integrated Circuits (RFIC) in September 2009. He served as a system engineer at Data Acquisition System (M) Sdn. Bhd. and tutor in USM. He is now a senior lecturer at the School of Electrical and Electronic Engineering, USM Engineering Campus. Mohd Tafir Mustaffa is a Senior Member of IEEE; actively involved with IEEE Circuits and Systems Society for the last few years as a committee member. He is the author and co-author of close to 50 technical papers in conferences and journals, books, and book chapters. He was a recipient of the IETE J C Bose Memorial Award in 2017. He is currently involved in the research of analog IC, RFIC, and RF MEMS design.



**Arjuna Marzuki** and graduated with B.Eng. in electronic engineering from the University of Sheffield, an MSc. from Universiti Sains Malaysia, and a Ph.D. degree from Universiti Malaysia Perlis. He was an associate professor at the School of Electrical and Electronic Engineering, Universiti Sains Malaysia. He is a professional engineer registered with the Board of Engineers Malaysia and a Chartered Engineer registered with the UK Engineering Council. He is also a Fellow of the Institution of Engineering and Technology (IET).